BMC Veterinary Research

RESEARCH

Open Access

Untargeted metabolomics analysis of the spleens of ducks infected with *Clostridium perfringens* type A

Chengrong Zeng[1,2,3], Na Wang[1,2], Ming Wen[1,2*], Bijun Zhou[1,2] and Ying Yang[1,2]

Abstract

Background The aim of this study was to investigate the metabolomic changes in the spleens of ducks artificially infected with *Clostridium perfringens* type A. Twenty-four healthy ducks aged 1 d were used for this purpose. After acclimatization for 37 d, the ducks were divided into 4 treatment groups ($n=6$): the control group (normal group), infection Group 1 (66 h), infection Group 2 (90 h) and infection Group 3 (114 h). The ducks in the corresponding infection group were challenged with 8 mL of *C. perfringens* type A bacterial solution (1×10^8 CFU/mL) for 4 days. The experimental ducks were culled at 0 h, 66 h, 90 h and 114 h after infection, and the ducks were sacrificed for spleen sampling at the end of the experiment. Autopsy observations, spleen pathological changes and pathogen nucleic acid detection were also performed. Finally, the changes in the metabolic profile of the spleen were investigated via a metabolomics approach.

Results At necropsy, the pathological changes in *C. perfringens* type A infection included enlarged, haemorrhagic and mottled spleens. Histopathology examination revealed that the ducks in the infection group had damaged spleen tissue structures, dilated spleen sinuses with congestion and bleeding, an extreme decrease in lymphocytes, and massive inflammatory cell infiltration in the splenic tissue. Spleen lesions were observed and PCR tests were positive in ducks in the infection group, indicating that a model of *C. perfringens* type A infection was successfully established in this study. Compared with those in the normal group, 14, 15 and 20 differentially abundant metabolites were identified after 66, 90 and 114 h, respectively, of *C. perfringens* type A infection of duck spleens, mainly including indolin-2-one, 3-methylindole, 4-hydroxy-2-quinolinecarboxylic acid, indole-3-methyl acetate, uric acid, 2'-deoxyinosine, urate, xanthine, 3-succinoylpyridine, nicotinic acid, phenylacetylglycine, histamine and phosphoenolpyruvate. Pathway analysis revealed that these metabolites were mainly involved in tryptophan metabolism, purine metabolism, nicotinate and nicotinamide metabolism, phenylalanine metabolism, histidine metabolism, phenylalanine, tyrosine and tryptophan biosynthesis, tyrosine metabolism, arginine and proline metabolism, arachidonic acid metabolism, and caffeine metabolism.

Conclusions These findings suggest that *C. perfringens* type A infection causes a duck spleen inflammatory response and immune response in infected ducks through indolin-2-one, 3-methylindole, 4-hydroxy-2-quinolinecarboxylic acid

*Correspondence:
Ming Wen
as.mwen@gzu.edu.cn

Full list of author information is available at the end of the article

and tryptophan metabolism, purine metabolism, nicotinic acid and nicotinamide metabolism, which provides a basis for understanding the pathogenesis of *C. perfringens* type A in ducks.

Keywords *Clostridium perfringens* type A, Duck, Spleen, Metabolic pathway

Background

Clostridium perfringens is a gram-positive, conditionally pathogenic bacterium that is common in the environment and causes food poisoning, intestinal disorders, and gas gangrene in both people and animals and is recognized as one of the most significant pathogens globally [1, 2]. According to the type of exotoxin they produce, *C. perfringens* can be divided into five serotypes, namely, types A, B, D, E, and F [3]. *C. perfringens* type A can widely infect livestock, poultry and humans, causing necrotizing enterocolitis and gas gangrene, which are extremely harmful [4]. Unfortunately, with the development of the duck farming industry, *C. perfringens* type A infection has become a widespread challenge. Numerous studies conducted in recent years have indicated that the prevalence of *C. perfringens* in duck farming has been increasing, with type A showing the highest prevalence and posing a severe danger to industry growth [5, 6]. However, the exact pathogenesis underlying *C. perfringens* type A has not yet been fully elucidated and the danger of *C. perfringens* in duck farming is growing. Changes in metabolites can provide new evidence to illustrate the disease pathogenesis, and nuclear magnetic resonance, gas chromatography-mass spectrometry, and liquid chromatography-tandem mass spectrometry are three major analytical platforms that are capable of capturing and mapping global metabolome composition and quantitative changes [7]. Liquid chromatography-tandem mass spectrometry, which is highly sensitive, adaptable, and does not require chemical derivatization, has emerged as a key technique for metabolomics research [8]. In addition, a previous study by our group revealed that *C. perfringens* type A-infected ducks had varying degrees of pathology at 66 h, 90 h, and 114 h (unpublished data). The faeces of healthy ducklings infected with *C. perfringens* type A for 0 h, 66 h, 90 h, and 114 h showed three-dimensional columnar, white urate porridge, white porridge with brown, and brown and tar-like in sequence; the duodenum also gradually developed diffuse intestinal haemorrhage from normal to haemorrhage accompanied by catarrhal inflammation and then acute catarrhal-haemorrhagic-necrotizing inflammation. However, few studies have been conducted on *C. perfringens* type A infecting duck spleens during these three time periods. Therefore, based on previous research LC-MS-based untargeted metabolomics was used to explore metabolites in the duck spleen and discriminate the metabolomic profile between *C. perfringens* type A-infected and noninfected duck spleens, as well as during the different stages of infection. In the study, we first established an experimental *C. perfringens* type A infection model in ducks and then used autopsies, histological analyses, and PCR test findings to demonstrate that the infection had been successful. Finally, changes in the metabolic profile of the spleens of ducks infected with *C. perfringens* type A were investigated via a metabolomics approach.

Results

Autopsy observation and pathological examination of the duck spleen

By observing the gross lesions of the spleen, it was found that the spleens of normal ducklings were bright red and oblate-ovate (Fig. 1A). When the ducklings were infected with *C. perfringens* type A for 66 h, the spleen was mottled (Fig. 1B). At 90 h after infection, the spleen was mildly enlarged with black haemorrhages under the mottled membrane (Fig. 1C). At 114 h after infection, the spleens of ducklings were mildly enlarged with mottled and more black haemorrhagic spots under the peritoneum (Fig. 1D). Compared with those of the controls, the splenic lesion scores were significantly greater ($P < 0.01$) at 66 h, 90 h and 114 h after infection (Fig. 3A). Pathological changes in the spleens of each group were analysed by HE staining, and it was found that the spleens of the normal control group had a clear histological structure and no lesions were observed (Fig. 2A). Compared with those in the control group, the splenic lymphocytes of the ducklings after 66 h of infection were dead, the cells were sparse, and no obvious splenic cell cord structure was observed (Fig. 2B). Spleen Sect. 90 h after infection showed a large number of erythrocytes with haemorrhagic infiltration, a large number of lymphocyte deaths and no obvious splenocyte cords (Fig. 2C). After 114 h of infection, splenic sections showed a large amount of inflammatory cell infiltration and haemorrhagic infiltration, and a large amount of red flocculent material formed by bruising was observed, with a large number of dead splenic lymphocytes and destruction of the cellular structure, with no obvious changes in the structure of the splenic cord (Fig. 3D). Compared with those of the control group, the Inflammatory lesion scores of the spleen were significantly greater at 66 h, 90 h and 114 h after infection ($P < 0.001$) (Fig. 3B).

PCR results for the duck spleen

The nucleic acid samples were tested for *C. perfringens* type A bacteria DNA via PCR. The findings demonstrated that none of the control spleen samples showed

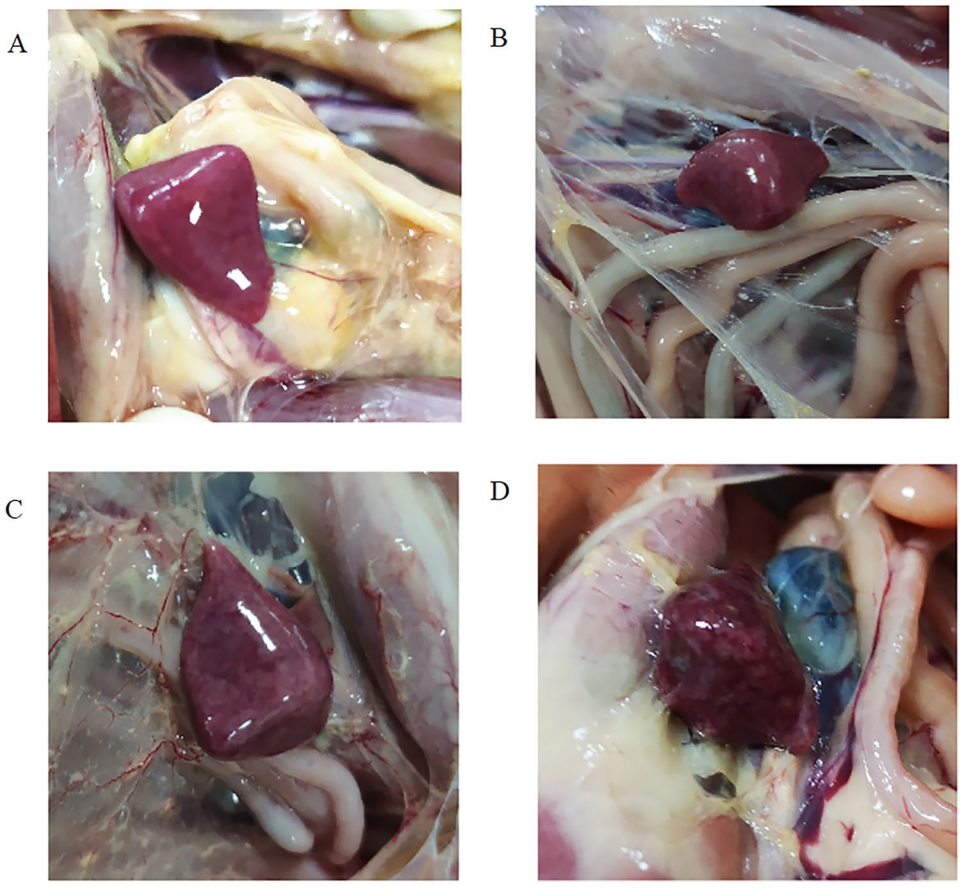

Fig. 1 Splenic dissection lesions in the control and three infected groups. Control group (**A**); Infection group 1 (**B**); Infection group 2 (**C**) and infection group 3 (**D**)

specific fragments of the expected fragment size. All Positive controls showed specific fragments that met expectations. Amplification of the target *C. perfringens* toxin gene fragment with a size of 507 bp in all infected groups was performed via 1.2% agarose gel electrophoresis. The results of sequence alignment showed that the homology between the infection group results and the reference genes was 99%. The results showed that none of the control ducks were infected with *C. perfringens* type A, while the spleens of the infected ducks were infected (Fig. 4).

Nontargeted metabolomics analysis of the spleen

In this study, spleen sample quality control analysis was performed using the body protection compound (BPC) superposition chart of all the QC sample spectrum detection charts (Supplementary Fig. 1), which indicated that the spectra overlapped well with small fluctuations in retention time and peak response intensity that the instrument was in good condition, and that the signal was stable throughout the sample detection and analysis and could be used for subsequent analysis.

To obtain the differentially abundant metabolites of the control and Infection groups, PCA and PLS-DA models were used. A PCA score plot of the control and Infection groups(66 h, 90 h and 114 h)is shown in Fig. 5. PCA of the processed data provides an overview of the plentiful metabolomics data of spleen samples, showing an obvious separation between control and infected spleen samples at three time points, of which a partial overlap occurred in some of the spleen samples, suggesting that the same ionic compounds may exist between the infected and control duck spleens. The statistical analysis of the differences in *C. perfringens* type A-infected duck spleen samples revealed that the four groups could be clearly distinguished from each other according to the PLS-DA models (Fig. 6). Overall, by integrating spleen samples, positive and negative ion modes, and PCA and PLS-DA analysis, the above results show that the metabolomics data are reliable and can be used for subsequent screening of differentials.

Differentially abundant metabolite screening

The *C. perfringens* type A spleen samples were screened for differentially abundant metabolites based on the PLS-DA model, where metabolites with p values < 0.05 and VIP > 1 in spleen samples were defined

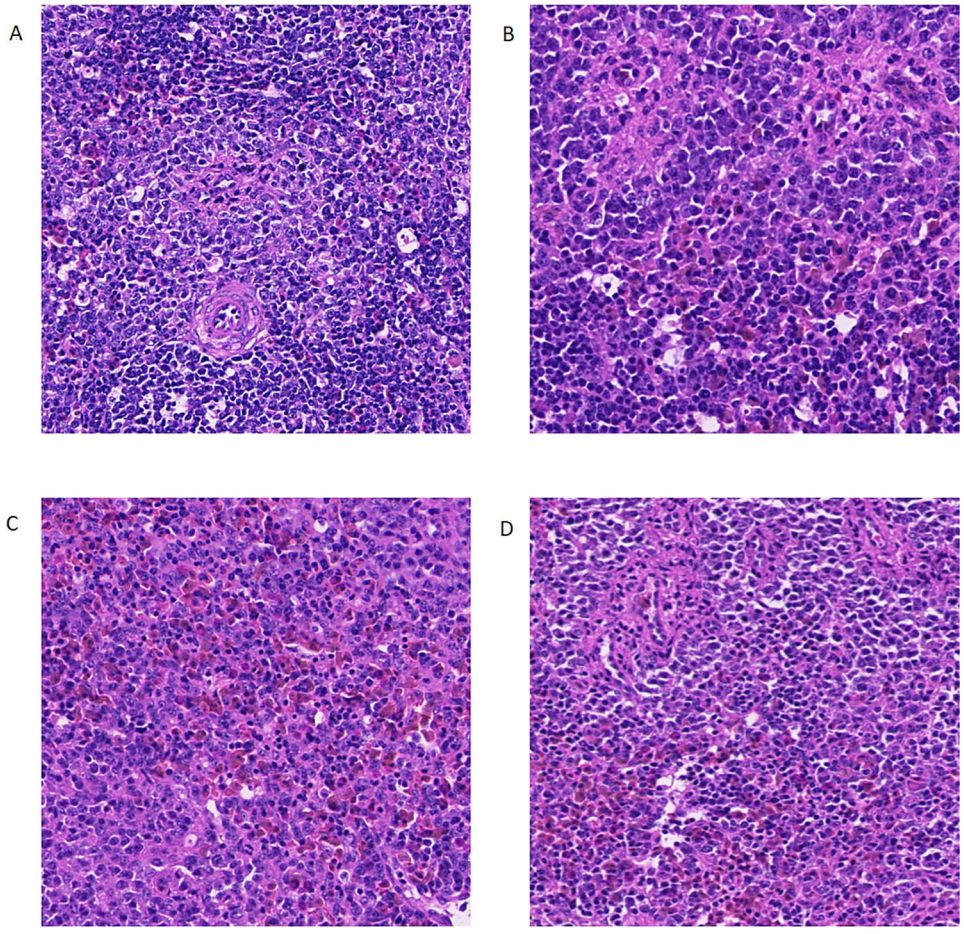

Fig. 2 Histological changes in spleen sections stained with HE in control and three Infection groups (200 £ magnification). Spleen tissue from control (**A**), infection group 1 (**B**), infection group 2 (**C**) and infection group 3 (**D**) by HE staining

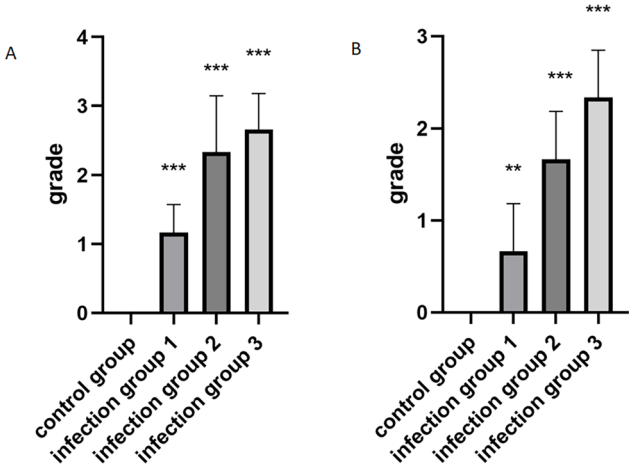

Fig. 3 Duck spleen lesion scoring. Spleen dissection lesion scoring graph (**A**) and spleen histological lesion scoring graph (**B**). All the data were presented as mean ± SD. '**' indicates P < 0.01, '***' indicates *P* < 0.001

as differentially abundant metabolites. Next, the differentially abundant metabolites between the normal group and three *C. perfringens* type A infection groups of duck spleen samples were visualized using volcano plots (Fig. 7). Seven differentially abundant metabolites were screened in positive ion mode at 66 h in infected ducks (Table 1), among which 1 was upregulated and 6 were downregulated. In negative ion mode, 7 differentially abundant metabolites were screened, among which 3 were upregulated, and 4 were downregulated. At 90 h after infection, there were a total of 15 differentially abundant metabolites (Table 1), including 10 differentially abundant metabolites in negative ion mode, of which 4 differentially abundant metabolites were upregulated and 6 differentially abundant metabolites were downregulated, and a total of 5 differentially abundant metabolites in positive ion mode, of which 3 were upregulated and 2 were downregulated. At 114 h after infection, there were a total of 20 differentially abundant metabolites (Table 1); 8 of these were in positive ion mode, where 3 were upregulated and 5 were downregulated, and 12 were in negative ion mode, where 1 was upregulated and 11 were downregulated.

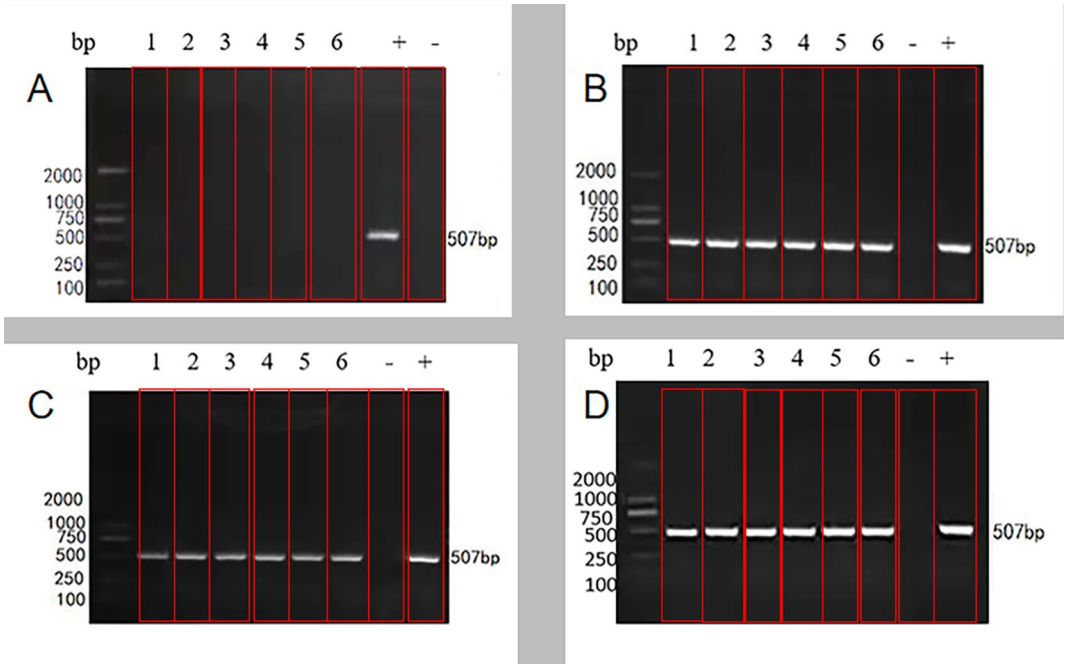

Fig. 4 Nucleic acid test results of *C. perfringens* type A infected duck pathogen. Spleen tissue from control group (**A**), infection group 1 (**B**), infection group 2 (**C**) and infection group 3 (**D**) by nucleic acid test

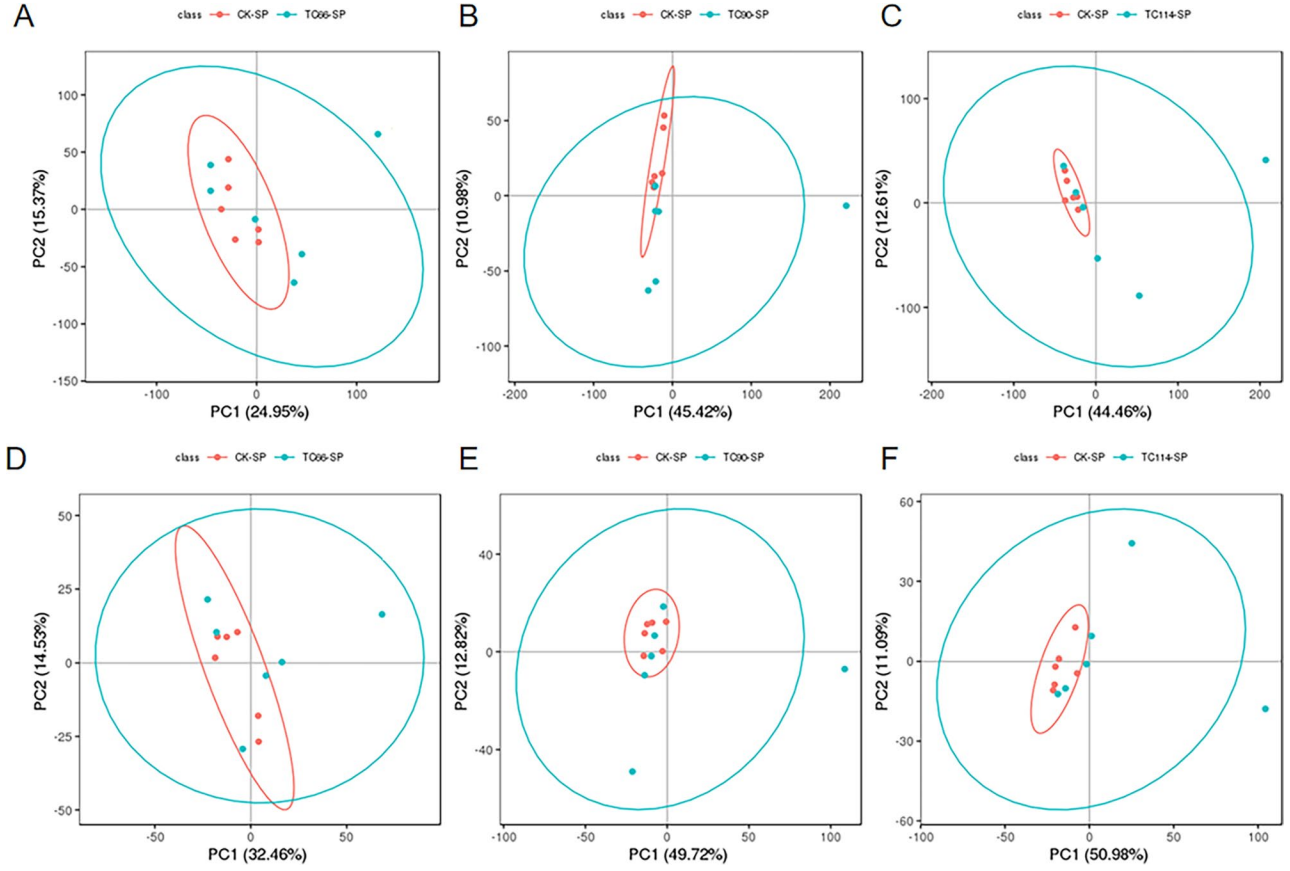

Fig. 5 PCA score plot of metabolomics assay in positive and negative ion mode. (**A** and **D**) PCA score plot between control and infection group 1 in positive and negative modes, (**B** and **E**) PCA score plot between control and infection group 2 in positive and negative modes, (**C** and **F**) PCA score plot between control and infection group 3 in positive and negative modes

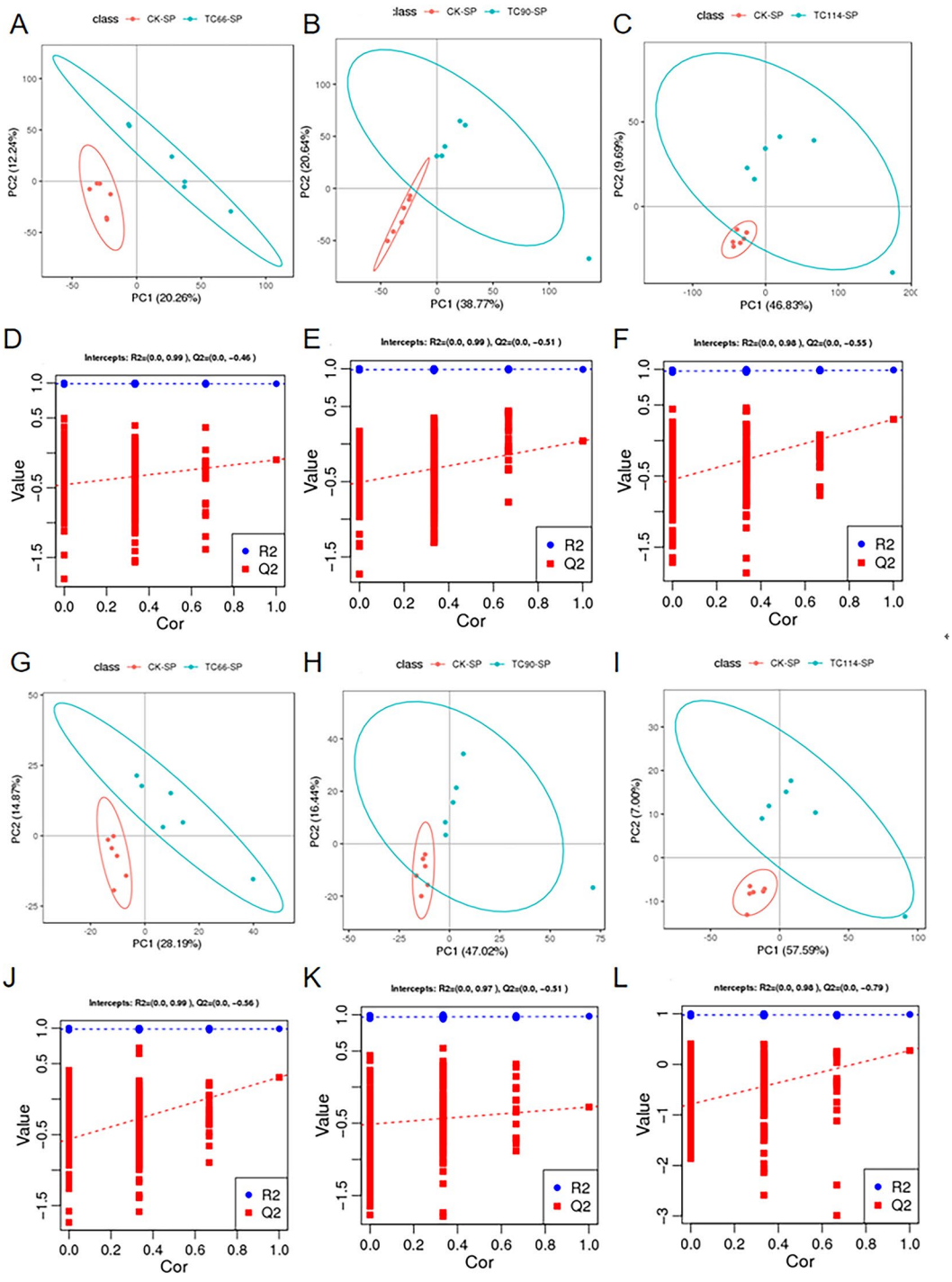

Fig. 6 PLS-DA score plots and permutation test derived from the spleen tissue of layers in control and three infection groups. (**A**-**C** and **G**-**I**) PLS-DA score plots between control and three infection groups in positive and negative modes, respectively. (**D**-**F** and **J**-**L**) Plot of the permutation test of PLS-DA modes in positive and negative modes, respectivel

Metabolic pathway analysis

To understand metabolic pathway changes in spleen samples from ducks infected with *C. perfringens* type A at different times, we conducted metabolic pathway enrichment analyses for differentially abundant metabolites in duck spleen samples based on the KEGG database. The results of the study showed that 10, 12 and 19 statistically significant metabolic pathways ($p < 0.05$) were enriched after infection for 66 h, 90 h and 114 h, respectively. A total of 10 metabolic pathways were identified

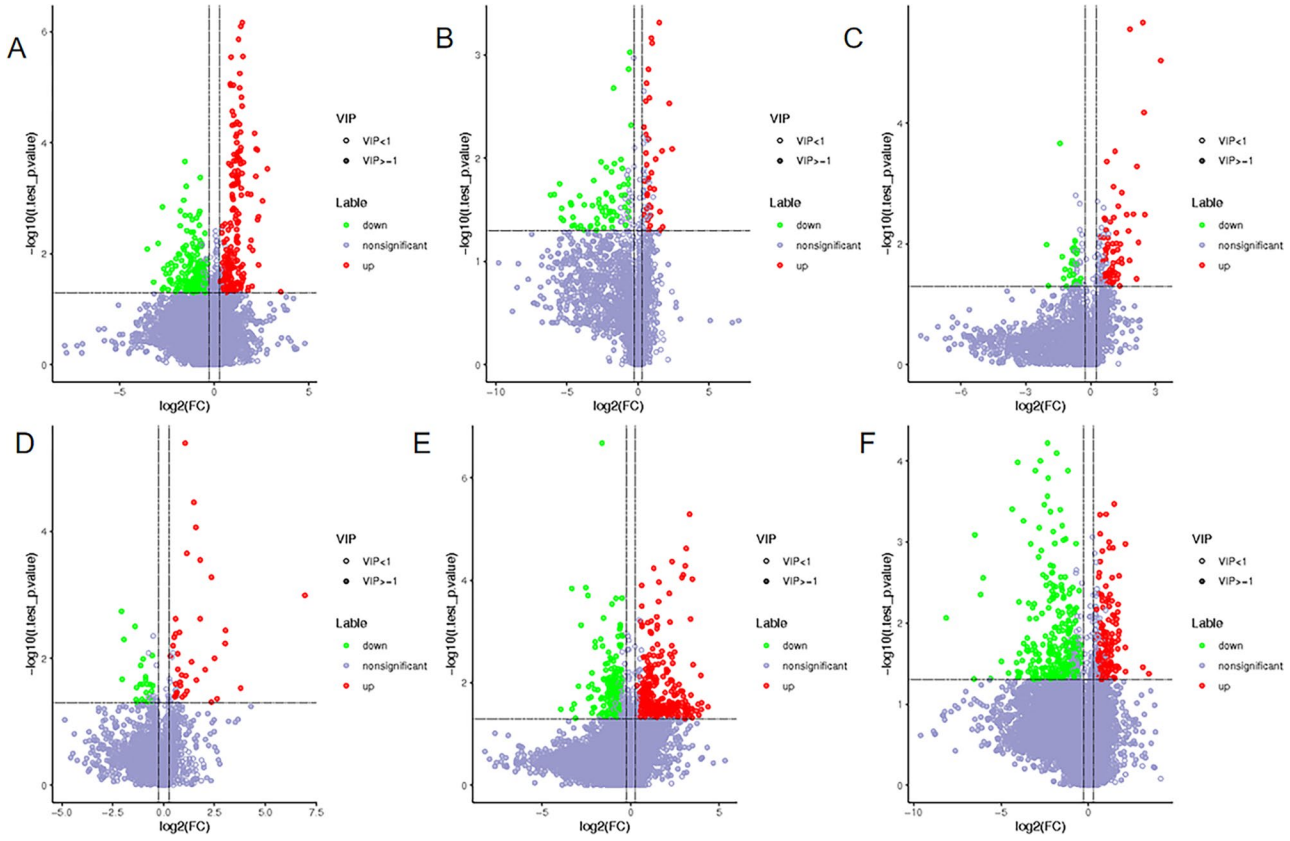

Fig. 7 Volcano plot of differential metabolites. Volcano plot was generated based on metabolites detected by the untargeted analysis in control group vs. infection group 1 in positive and negative modes (**A** and **D**), control group vs. infection group 2 (**B** and **E**) and control group vs. infection group 3 (**C** and **F**). The red nodes represent significantly up-regulated metabolites, green nodes represent significantly down-regulated metabolites, respectively. The grey modes represent metabolites with no significance

at 66 h of infection, 5 each in positive and negative ion modes. In positive ion mode, splenic differentially abundant metabolites were mainly enriched in tryptophan metabolism, purine metabolism, nicotinate and nicotinamide metabolism, metabolic pathways, and adrenergic signalling in cardiomyocytes; in the negative ion mode, splenic differentially abundant metabolites were mainly enriched in pyrimidine metabolism, purine metabolism, phenylalanine metabolism, metabolic pathways, drug metabolism-other enzymes (Fig. 8). A total of 12 metabolic pathways were enriched at 90 h after infection. In the positive ionization mode, splenic differentially abundant metabolites were mainly enriched in pyrimidine metabolism, histidine metabolism, arginine and proline metabolism, and in the negative ionization mode, splenic differentially abundant metabolites were mainly enriched in pyruvate metabolism, pyrimidine metabolism, phosphonate and phosphinate metabolism, phenylalanine, tyrosine and tryptophan biosynthesis, the pentose phosphate pathway, metabolic pathways, glycolysis/gluconeogenesis, the citrate cycle (TCA cycle), and carbon metabolism (Fig. 8). In contrast, 19 metabolic pathways were identified at 114 h of infection, and in the positive ion mode, splenic differentially abundant metabolites were mainly enriched in tyrosine metabolism, tryptophan metabolism, phenylalanine metabolism, nicotinate and nicotinamide metabolism, neuroactive ligand-receptor interaction, metabolism of xenobiotics by cytochrome P450, metabolic pathways, gap junction, C-type lectin receptor signalling pathway and arachidonic acid metabolism; in the negative ion mode, splenic differentially abundant metabolites were mainly enriched in tryptophan metabolism, PPAR signalling pathway, phenylalanine metabolism, nicotinate and nicotinamide metabolism, neuroactive ligand-receptor interaction, metabolic pathways, coffee metabolism, arachidonic acid metabolism, and alpha-linolenic acid metabolism (Fig. 8).

Discussion

C. perfringens is an important pathogen in livestock and poultry farming that is widely distributed in the human and animal gastrointestinal tract, decaying vegetation, soil, manure and other environments and can cause food poisoning in humans and gastroenteritis in animals [9, 10]. The harm caused by *C. perfringens* is the most severe of these. *C. perfringens* type A infection in ducks has been

Table 1 The significantly differential metabolites in positive and negative ion mode

Nos	Metabolites	VIP	*p*-value	label	Ion mode
Infection 66 h spleen differential metabolites					
1	Cytidine	1.3113	0.5166	∃	pos
2	Uric acid	2.1355	0.5047	#	pos
3	2′-Deoxyinosine	2.0203	0.2814	∃	pos
4	Hexanoylcarnitine	1.8748	0.4631	∃	pos
5	indolin-2-one	2.2005	0.524	∃	pos
6	3-succinyl pyridine	1.424	0.5095	∃	pos
7	N-diphenylurea	3.4782	0.3026	∃	pos
8	3-Hydroxybutyric acid	3.2941	0.0001	#	neg
9	Cytidine	1.5316	0.0254	∃	neg
10	Uridine	1.1552	0.0481	∃	neg
11	3-Hydroxymandelic acid	4.2784	0.01	#	neg
12	N-Acetyl-d-isoleucine	1.124	0.0046	#	neg
13	Uric acid salt	1.2418	0.0216	∃	neg
14	N, n′-diphenylurea	2.4408	0.0129	∃	neg
Infection 90 h spleen differential metabolites					
1	Phosphoenolpyruvic acid	2.7643	0.0001	#	pos
2	3-Hydroxybutyric acid	4.0802	0	#	pos
3	Cytidine	1.1104	0.0131	∃	pos
4	Hexadecanedioic acid	2.003	0.0036	#	pos
5	Methylhydroxyprogesterone	1.1206	0.0274	∃	pos
6	Histamine	1.7855	0.0443	∃	neg
7	N8-Acetyl spermidine	2.1788	0.0019	∃	neg
8	Cytosine	1.0688	0.0098	∃	neg
9	Cytidine	1.1247	0.0166	∃	neg
10	N6-Acetyl-1-lysine	1.219	0.0182	#	neg
11	3-Methylindole	1.8123	0.0442	#	neg
12	Hexanoylcarnitine	1.3697	0.0183	∃	neg
13	N, n′-diphenylurea	1.1618	0.0261	∃	neg
14	Hexadecanedioic acid	2.0611	0.0268	#	neg
15	Isophorone	2.7643	0.0001	#	neg
Infection 144 h spleen differential metabolites					
1	Dl-4-hydroxyphenyl lactic acid	1.1537	0.0325	∃	pos
2	Nicotinic acid	1.3383	0.0081	∃	pos
3	Xanthine	1.4775	0.0008	#	pos
4	3-Hydroxymandelic acid	3.6822	0.0328	#	pos
5	2,4-Dihydroxybenzoic acid	2.6039	0.0496	#	pos
6	Methyl nicotinoylacetate	1.1204	0.0103	∃	pos
7	Retinol	1.1718	0.024	∃	pos
8	12-Octadecadienoic acid	2.4223	0.0125	∃	pos
9	Putrescine	1.3309	0.6884	∃	neg
10	N8-acetyl spermidine	2.7392	0.4031	∃	neg
11	o-Acetylcarnitine	1.189	0.7091	∃	neg
12	N-Acetyl proline	1.048	0.6899	∃	neg
13	Dopamine	1.8822	0.011	∃	neg
14	4-hydroxy-2-quinolinecarboxylic acid	1.8919	0.088	∃	neg
15	Phenylacetylglycine	2.3893	0.3484	∃	neg
16	Hexanoylcarnitine	1.728	0.4419	∃	neg
17	Penicillin	6.2903	0.0913	∃	neg
18	Indole-3-methyl acetate	1.1104	0.4007	∃	neg
19	3-Succinyl pyridine	1.2845	0.4516	∃	neg
20	Bilirubin	1.4035	0.5238	#	neg

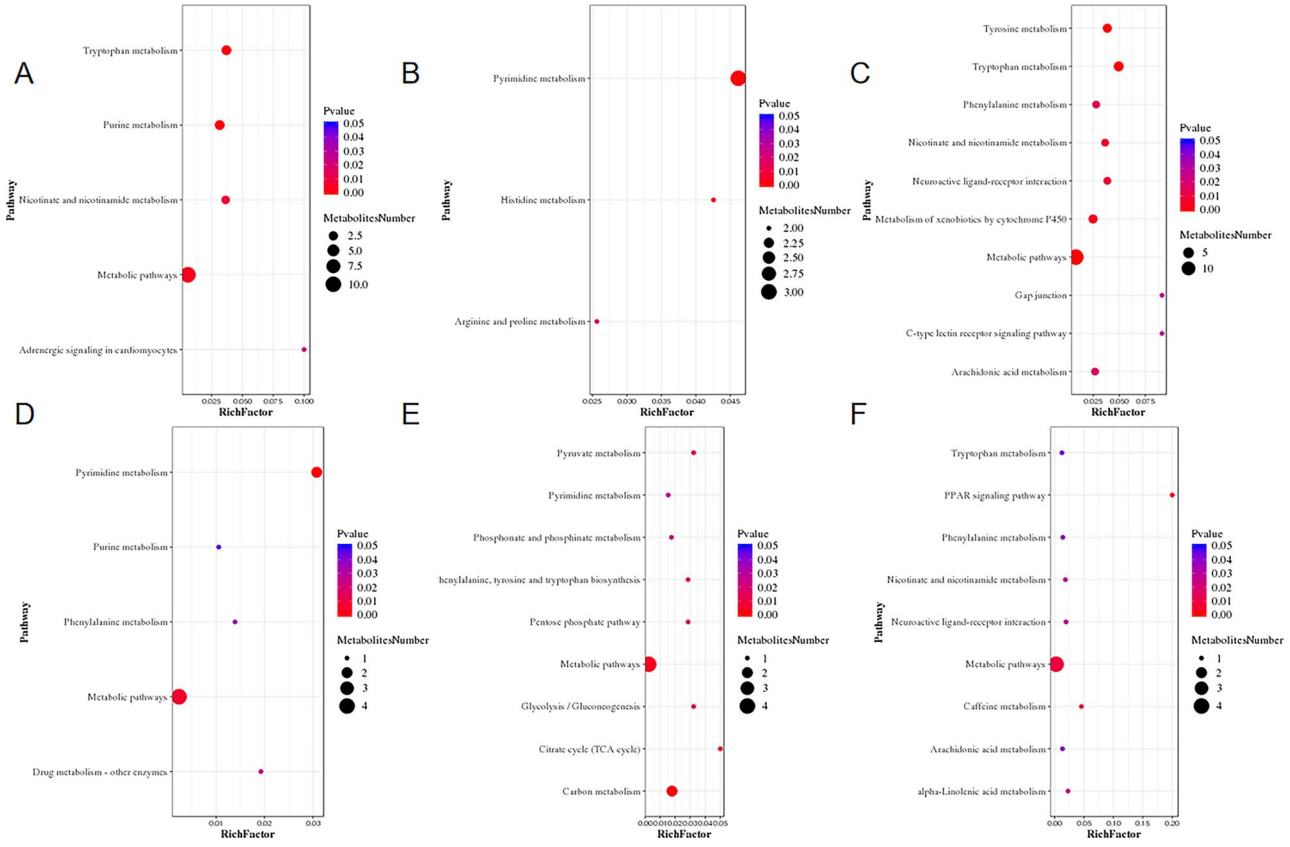

Fig. 8 KEGG enrichment bubble diagram. (**A** and **D**) Pathway analysis between control and infection group 1 in positive and negative modes, (**B** and **E**) Pathway analysis between control and infection group 2 in positive and negative modes, (**C** and **F**) Pathway analysis between control and infection group 3 in positive and negative modes

observed in several places in recent years, resulting in significant financial losses for the duck farming industry. Liu et al. [11] investigated and tracked *C. perfringens* type A strains from three duck farms by isolating 334 strains from 788 samples, 316 (94.61%) of which were type A strains. However, the pathogenesis of *C. perfringens* type A remains unclear. The spleen is the largest peripheral lymphoid organ in ducks and plays an important role in the immune response of the body, which protects the body from microbial invasion and direct resistance to external infections [12, 13]. Transcriptome sequencing by Truong et al. [14] revealed that necrotizing enterocolitis in chickens led to the upregulation of JAK, TYK2, STAT, SOCS1, SOCS2, SOCS4, SOCS5, IFN-α and IL gene expression in spleen tissue. In that respect, nontargeted metabolomics has shown significant potential in describing the changes in *C. perfringens*-infected chickens, but very few nontargeted studies have actually analysed the changes in *C. perfringens* type A-infected duck spleens at different times. Therefore, to establish an experimental infection model for *C. perfringens* type A in ducks, it is crucial to use autopsy observation, pathological examination and PCR testing to determine the success of the infection. Finally, the changes in the metabolic profile of the spleen were investigated with the application of a nontargeted metabolomics approach. At 66 h, 90 h and 114 h, respectively, 14, 15, and 20 differentially abundant metabolites, respectively were found in the spleens of infected ducks, including indolin-2-one, 3-methylindole, 4-hydroxy-2-quinolinecarboxylic acid, indole-3-methyl acetate, uric acid, 2'-deoxyinosine, urate, xanthine, 3-succinoylpyridine, nicotinic acid, phenylacetylglycine, histamine and phosphoenolpyruvate, which are thought to be associated with the mechanism of *C. perfringens* type A infection. The KEGG pathway enrichment analysis revealed that these metabolites were involved mainly in tryptophan metabolism, purine metabolism, nicotinate and nicotinamide metabolism, phenylalanine metabolism, histidine metabolism, phenylalanine, tyrosine and tryptophan biosynthesis, tyrosine metabolism, arginine and proline metabolism, arachidonic acid metabolism, and caffeine metabolism.

Tryptophan is an essential amino acid for poultry, is required for protein formation, and plays vital roles in the nervous, endocrine, intestinal and immune systems, where it has a powerful effect on both innate and adaptive immunity [15, 16]. As an important immunomodulatory effect, there are three main pathways of tryptophan

metabolism, and all three pathways can act simultaneously: [1] by depleting tryptophan and making tryptophan-dependent cells deficient in essential amino acids [2], by affecting the production of bioactive proteins, and [3] by regulating immune cell metabolism [17]. Liu et al. [18] reported that the administration of tryptophan to a poultry diet can significantly increase the serum total antioxidant capacity and glutathione peroxidase and catalase levels while alleviating stress and improving growth performance and meat quality. In addition, Mund et al. [19] reported that supplementation with tryptophan improved the growth performance, antioxidant status, and immune function of broilers. In this study, the metabolites indolin-2-one, 3-methylindole, 4-hydroxy-2-quinolinecarboxylic acid, and indole-3-methyl acetate showed significant changes after *C. perfringens* type A infection, and they were mainly involved in two metabolic pathways—tryptophan metabolism and phenylalanine, tyrosine, and tryptophan biosynthesis—suggesting that infected ducks may experience exacerbated inflammatory and immune responses through modulation of tryptophan metabolic pathways and alanine, tyrosine, and tryptophan biosynthesis. In addition to tryptophan metabolism, purine metabolism was significantly enriched in this assay. The most abundant metabolic substrates for all organisms are purines, which are crucial for the synthesis of DNA and RNA and play a crucial role in controlling the innate immune system and inflammatory response [20–22]. Purine not only acts as a metabolic substrate for inhibiting xanthine oxidoreductase for uric acid production but also induces inflammation through IFN-γ secretion which stimulates uric acid production through the attenuation of xanthine oxidoreductase expression [23]. Kuo et al. [24] discovered that purine metabolic mechanisms may balance the demand and supply of ATP in shrimp to tolerate environmental or pathogen-induced stress. Additionally, Wu et al. [25] reported that rhubarb acid could decrease uric acid concentrations, which indirectly changed purine metabolism in the intestine, modulated the gut microbiota and subsequently alleviated chronic colitis. Notably, significant changes in the concentrations of several metabolites (uric acid, 2'-deoxyinosine, urate and xanthine) related to purine metabolism were observed in this study, such as significant increases in uric acid occurring, suggesting that *C. perfringens* type A infection of the duck spleen may cause an inflammatory response by affecting purine metabolism and related metabolites.

In addition, in the present study, the nicotinate and nicotinamide metabolism pathways were also significantly enriched. Nicotinic acid and nicotinamide, which are also called vitamin B3, act as two precursors to biologically active coenzymes, nicotinamide adenine dinucleotide phosphate (NADP) and nicotinamide adenine dinucleotide (NAD) [26, 27]. These two coenzymes participate in redox reactions necessary for energy production, and the pyridine ring can absorb and give rise to a hydride ion, which acts in the cytoplasm with a different metabolic capacity as an electron carrier [28]. In the inflammatory response, reduced nicotinamide adenine dinucleotide phosphate (NADPH) is a substrate for NADPH oxidases which are used by neutrophils and phagocytes to inactivate microorganisms by producing superoxide free radicals [29]. Many studies have shown that high stocking density rearing may increase the risk of muscle disorders; dietary supplementation with nicotinamide (NAM) and butyrate sodium (BA) may improve chicken muscle quality by enhancing antioxidant capacity, inhibiting protein ubiquitination and the inflammatory response, and upregulating the expression of myogenic genes [30, 31]. Guo et al. [32] reported that niacin could reduce the inflammatory response of BMECs through GPR109A/AMPK/NRF-2/autophagy and alleviate the effects of mastitis in cows. In this study, the levels of the metabolites 3-succinoylpyridine and nicotinic acid significantly changed after *C. perfringens* type A infection, and these metabolites are involved mainly in nicotinate and nicotinamide metabolism which infected ducks may cause inflammatory responses in infected ducks by affecting the nicotinate and nicotinamide metabolism pathways. It is well known that histidine is an essential amino acid in mammals, fish and poultry and is considered promising for the prevention and treatment of metabolic syndrome, dermatitis, ulcers and inflammatory bowel disease [33, 34]. Whereas histamine, the major metabolite of the histidine metabolic pathway, is mostly synthesized and stored in granules in mast cells and basophils and is released through degranulation induced by immunological stimulation to the extent that feeding histidine affects histamine concentrations in immune cells, insufficient histidine intake decreases histamine levels and affects organismal immunity [35]. In the present study, the histamine levels also decreased significantly, suggesting that *C. perfringens* type A infection ducks may lead to reduced immunity and inflammation in the organism by affecting histamine levels in the histidine metabolic pathway. In addition, numerous metabolites were also significantly enriched for tyrosine metabolism, phenylalanine metabolism, arachidonic acid metabolism, arginine and proline metabolism, and caffeine metabolism pathways, all of which are associated with immunity and inflammation in the ducks.

Conclusions

In conclusion, in this study we established a model of *C. perfringens* infection, used necropsy, pathological examination, and PCR to determine successful infection, and then performed nontargeted metabolomics analysis to

examine the changes in metabolites and metabolic pathways of *C. perfringens* type A after infection of the spleen of ducks at various times. The results showed that *C. perfringens* type A infection of the duck spleen mainly affects splenic inflammation and the immune response by affecting indolin-2-one, 3-methylindole, 4-hydroxy-2-quinolinecarboxylic acid, uric acid, 2'-deoxyinosine, urate, xanthine, nicotinic acid, 3-succinylpyridine and tryptophan metabolism, purine metabolism, and nicotinate and nicotinamide metabolism, which provides a new direction for understanding the pathogenesis of *C. perfringens* type A from the perspective of spleen metabolites.

Methods

Experimental animals and strains

The *C. perfringens* type A standard strain (CVCC2030) was purchased from the China Institute of Veterinary Drug Control. A total of 24 one-day-old ducks were purchased from Guangdong Mingyan Poultry Co.

Establishment of a *C. perfringens* type a artificially infected duck model

At 36 d after the rear, the ducks were randomly divided into 4 groups ($n=6$ ducks per group): a control group without infection (inoculated with physiological saline) and 3 infection groups (66 h, 90 h and 114 h), in which the ducks were orally inoculated via gavage at 37 d of age with 8 mL of a PBS suspension containing the *C. perfringens* type A reference strain CVCC2030(1×10^8 CFU/mL) once daily for 4 d. All the experimental procedures were approved by the Experimental Animal Ethics Committee of Guizhou University (No: EEA-GZU-2022-TO17) in accordance with the Guiding Principles for the Care and Use of Laboratory Animals (China).

Sample collection

The spleens of the ducks in each group were collected at 66 h, 90 h and 144 h after model establishment. A portion of spleen tissue was fixed in 4% formalin for observation of pathological changes, and the remaining spleen tissue was snap-frozen in liquid nitrogen and then stored at -80 °C for metabolomics analysis.

Autopsy observation and pathological examination

At the end of the experiment, the ducks were euthanized by intravenous administration of sodium pentobarbital (100 mg/kg body weight) and then the abdominal and thoracic cavities were opened for observation and collection of gross lesions in the splenic tissue. Splenic lesions were scored as described by Wang et al. [36]. Under the standard protocol, spleen tissues were formalin-fixed, paraffin-embedded, sectioned, and stained with haematoxylin and eosin (HE) [37]. HE-stained sections were examined using a biological microscope. Each slide was evaluated on a blinded basis and scored through three grades, according to the methods described by Arafat et al. [38].

Table 2 Sequence of PCR primer

GeneBank No	Primer name	Primer sequence (5′~3′)	Primer size/bp
X17300.1	CpA -α	F: TGTAAGGCGCTTGTTTGTGC R: TGCGCTATCAACGGCAGTAA	507

C. perfringens type a nucleic acid assay

Primers were designed according to the gene sequence of *C. perfringens* type A in GenBank, and the specific primer information is shown in Table 2. The primers were synthesized by Bioengineering (Shanghai) Co. *C. perfringens* type A bacterial fluid was used as a positive control. DNA samples were extracted from the spleens of control and infected ducks using the DNA extraction kit, and the extracted DNA was used as the template for PCR amplification to detect the *C. perfringens* type A α toxin gene. The PCR amplification system included 12.5 μL of 2×Taq PCR Master Mix, 1 μL each of the upstream and downstream primers (10 μmol/L), 2 μL of template, and 8.5 μL of ddH2O. The reaction cycles were performed as follows: 94 °C for 5 min; 30 cycles at 94 °C for 30 s, 57 °C for 30 s, and 72 °C for 30 s; and 72 °C for 10 min.

Spleen metabolite extraction

Six spleen samples from each group were selected and thawed at 4 °C. Then, 25 mg of splenic tissue was precisely weighed, and 800 μL of cold methanol/acetonitrile/water (2:2:1, v/v/v) was added. Then the samples were homogenized at 50 Hz for 5 min and sonicated for 10 min in an ice-water bath. After centrifugation at 25 000 rpm for 15 min at 4 °C, all the supernatant was transferred to another 600 μL centrifuge tube and concentrated to dryness under vacuum. The samples were redissolved in 200 μL of methanol/water (1:9, v/v) for metabolomic analysis. Quality control (QC) samples pooled from all spleen tissue samples were prepared and analysed via the same procedure.

LC-MS analysis

LC-MS analyses were performed using a Q Exactive HF high-resolution mass spectrometer (Thermo Fisher Scientific, USA) equipped with a Waters 2D UPLC (1.7 μm 2.1*100 mm, Waters, USA) column maintained at 45 °C. The column was eluted at a flow rate of 0.35 mL/min. The mobile phase consisted of A (0.1% formic acid in water and 10 mM ammonium formate) and B (0.1% formic acid in water and 10 mM ammonium formate) with the following gradient: 0–1 min, 2% B; 1–9 min, 2-98% B; 9–12 min, 98% B; 12–12.1 min, 98%-2% B; and 12.1–15 min, 2% B.

The mass spectrometry data were acquired by a Q Exactive HF mass spectrometer for primary and secondary mass spectrometry. In ionization mode, mass spectral metabolomics data from duck spleen samples were collected with a mass range of 70–1050 m/z. The primary resolution was 120,000, and the secondary resolution was 30,000. The parameters of the polarity of the ESI were as follows: the flow rates of the sheath gas and auxiliary gas were 40 and 10, respectively; the temperatures of the capillary and auxiliary gas heater were set at 320 °C and 350 °C respectively: the negative ion spray voltage was 3.2 kV: and the positive ion spray voltage was 3.80 kV.

Metabolite identification and pathway analysis

Partial least squares discriminant analysis (PLS-DA) and principal component analysis (PCA), combined with t test to obtain p values (VIP > 1, $P < 0.05$), were performed to identify potentially differentially abundant metabolites between normal and *C. perfringens* type A-infected ducks at different times. In addition, to judge the model quality, the PLS-DA model was subjected to 200 response permutation tests (RPTs). To explore the metabolites associated with *C. perfringens* type A infection of duck spleens at different times, we used the Human Metabolome Database (HMDB, http://www.hmdb.ca/) to analyse the potential biomarker metabolites. Metabolic pathway enrichment analysis of differentially abundant metabolites in the spleens of normal and infected ducks was performed based on the KEGG database. Significantly enriched pathways with p value less than 0.05 according to the p value of the hypergeometric test were identified as those with significant enrichment of differentially abundant metabolites.

Data processing and analysis

LC–MS/MS raw mass spectrometry data (raw files) were processed using Compound Discoverer 3.1 (Thermo Fisher Scientific, United States), which included retention time correction within and between groups, peak extraction, additive ion pooling, background peak labelling, missing value filling, and metabolite identification before being exported. Then, for data preprocessing, the retention time, compound molecular weight, and peak area information was imported into metaX. Probabilistic quotient normalization (PQN) was used to normalize the data to primarily obtain the relative peak regions. Batch effects were corrected using QC-RLSC, a quality control-based robust LOESS signal correction method. All quality control samples were free of any compounds with a coefficient of variation (CV) greater than 30% of the relative peak area. The relationship between metabolite expression and sample categories was modelled using PCA and PLS-DA, which assisted in predicting sample categories. Fold changes and Student's t test were subsequently applied to determine the differentially abundant metabolites between the control group and the three infected groups.

Abbreviations

HE	Hematoxylin and eosin
PQN	The Probabilistic Quotient Normalization
CV	Coefficient of variation
PLS-DA	Partial least squares discriminant analysis
PCA	Principal component analysis
RPT	Response permutation tests
QC	Quality control

Supplementary Information

The online version contains supplementary material available at https://doi.org/10.1186/s12917-025-04539-9.

Supplementary Material 1

Acknowledgements

We are grateful to all reviewers and editors who participated in the preparation of this manuscript for their linguistic assistance.

Author contributions

M.W., B.Z., Y.Y. and N.W. conceived the study; C. Z. and N. W. performed the experiments; C. Z. wrote the main manuscript and analysed the data. All authors have read and agreed to the published version of the manuscript.

Funding

This work was supported by the Guizhou High-Level Innovative Talents Training "Hundred Level Innovative Talents" (Qiankehe Talents [2016] No. 4009). The author is very thankful for the financial support.

Data availability

The data will be made available upon request.

Declarations

Ethics approval and consent to participate

The experimental protocols used in this study, including animal breeding, care and use, were reviewed and approved by the Animal Care and Use Ethics Committee of Guizhou University (EAE-GZU-2022-TO17). All methods were carried out in accordance with relevant guidelines and regulations and were reported in accordance with ARRIVE guidelines for the reporting of animal experiments.•.

Consent for publication

Not applicable.

Competing interests

The authors declare no competing interests.

Author details

[1]College of Animal Science, Guizhou University, Guiyang 550025, China
[2]Key Laboratory of Animal Diseases and Veterinary Public Health of Guizhou Province, College of Animal Science, Guizhou University, Guiyang 550025, China
[3]Weining County Animal Prevention Control enter, Bijie 553100, China

Received: 31 October 2023 / Accepted: 29 January 2025
Published online: 29 April 2025

References

1. Kiu R, Hall LJ. An update on the human and animal enteric pathogen Clostridium perfringens. Emerg Microbes Infect. 2018;7(1):141.

2. Rood JI, Adams V, Lacey J, Lyras D, McClane BA, Melville SB, et al. Expansion of the Clostridium perfringens toxin-based typing scheme. Anaerobe. 2018;53:5–10.
3. Llanco LA, Nakano V, Moraes CTP, Piazza RMF, Avila-Campos MJ. Adhesion and invasion of Clostridium perfringens type a into epithelial cells. Braz J Microbiol. 2017;48(4):764–8.
4. Navarro MA, Li J, Beingesser J, McClane BA, Uzal FA. The Agr-Like Quorum-Sensing System is important for Clostridium perfringens type a strain ATCC 3624 to cause gas gangrene in a mouse model. mSphere. 2020;5(3).
5. Xiu L, Liu Y, Wu W, Chen S, Zhong Z, Wang H. Prevalence and multilocus sequence typing of Clostridium perfringens isolated from 4 duck farms in Shandong province, China. Poult Sci. 2020;99(10):5105–17.
6. Liu Y, Xiu L, Miao Z, Wang H. Occurrence and multilocus sequence typing of Clostridium perfringens isolated from retail duck products in Tai'an region, China. Anaerobe. 2020;62:102102.
7. Cui L, Lu H, Lee YH. Challenges and emergent solutions for LC-MS/MS based untargeted metabolomics in diseases. Mass Spectrom Rev. 2018;37(6):772–92.
8. Chaleckis R, Meister I, Zhang P, Wheelock CE. Challenges, progress and promises of metabolite annotation for LC-MS-based metabolomics. Curr Opin Biotechnol. 2019;55:44–50.
9. Yadav JP, Das SC, Dhaka P, Vijay D, Kumar M, Mukhopadhyay AK, et al. Molecular characterization and antimicrobial resistance profile of Clostridium perfringens type a isolates from humans, animals, fish and their environment. Anaerobe. 2017;47:120–4.
10. Mehdizadeh Gohari I, M AN, Li J, Shrestha A, Uzal F. Pathogenicity and virulence of Clostridium perfringens. Virulence. 2021;12(1):723–53.
11. Liu L, Wang H, Xu W, Yin Y, Ren Y, Bu H, et al. Tracking Clostridium perfringens strains from breeding duck farm to commercial meat duck farm by multilocus sequence typing. Vet Microbiol. 2022;266:109356.
12. Xu M, Li W, Yang S, Sun X, Tarique I, Yang P, et al. Morphological characterization of postembryonic development of blood-spleen barrier in duck. Poult Sci. 2020;99(8):3823–30.
13. Wan F, Tang L, Rao G, Zhong G, Jiang X, Wu S, et al. Curcumin activates the Nrf2 pathway to alleviate AFB1-induced immunosuppression in the spleen of ducklings. Toxicon. 2022;209:18–27.
14. Truong AD, Rengaraj D, Hong Y, Hoang CT, Hong YH, Lillehoj HS. Differentially expressed JAK-STAT signaling pathway genes and target microRNAs in the spleen of necrotic enteritis-afflicted chicken lines. Res Vet Sci. 2017;115:235–43.
15. Zhang YN, Ruan D, Wang S, Huang XB, Li KC, Chen W, et al. Estimation of dietary tryptophan requirement for laying duck breeders: effects on productive and reproductive performance, egg quality, reproductive organ and ovarian follicle development and serum biochemical indices. Poult Sci. 2021;100(8):101145.
16. Tsuji A, Ikeda Y, Yoshikawa S, Taniguchi K, Sawamura H, Morikawa S et al. The Tryptophan and Kynurenine Pathway involved in the development of Immune-Related diseases. Int J Mol Sci. 2023;24(6).
17. Fiore A, Murray PJ. Tryptophan and indole metabolism in immune regulation. Curr Opin Immunol. 2021;70:7–14.
18. Liu Y, Yuan JM, Zhang LS, Zhang YR, Cai SM, Yu JH, et al. Effects of tryptophan supplementation on growth performance, antioxidative activity, and meat quality of ducks under high stocking density. Poult Sci. 2015;94(8):1894–901.
19. Mund MD, Riaz M, Mirza MA, Rahman ZU, Mahmood T, Ahmad F, et al. Effect of dietary tryptophan supplementation on growth performance, immune response and anti-oxidant status of broiler chickens from 7 to 21 days. Vet Med Sci. 2020;6(1):48–53.
20. Huang Z, Xie N, Illes P, Di Virgilio F, Ulrich H, Semyanov A, et al. From purines to purinergic signalling: molecular functions and human diseases. Signal Transduct Target Ther. 2021;6(1):162.
21. Yin J, Ren W, Huang X, Deng J, Li T, Yin Y. Potential mechanisms connecting Purine Metabolism and Cancer Therapy. Front Immunol. 2018;9:1697.
22. Liu J, Hong S, Yang J, Zhang X, Wang Y, Wang H, et al. Targeting purine metabolism in ovarian cancer. J Ovarian Res. 2022;15(1):93.
23. Wang H, Xie L, Song X, Wang J, Li X, Lin Z, et al. Purine-Induced IFN-gamma promotes uric acid production by upregulating Xanthine Oxidoreductase expression. Front Immunol. 2022;13:773001.
24. Kuo CH, Ballantyne R, Huang PL, Ding S, Hong MC, Lin TY, et al. Sarcodia suae modulates the immunity and disease resistance of white shrimp Litopenaeus vannamei against Vibrio alginolyticus via the purine metabolism and phenylalanine metabolism. Fish Shellfish Immunol. 2022;127:766–77.
25. Wu J, Wei Z, Cheng P, Qian C, Xu F, Yang Y, et al. Rhein modulates host purine metabolism in intestine through gut microbiota and ameliorates experimental colitis. Theranostics. 2020;10(23):10665–79.
26. Nikas IP, Paschou SA, Ryu HS. The role of Nicotinamide in Cancer Chemoprevention and Therapy. Biomolecules. 2020;10(3).
27. Campbell JM. Supplementation with NAD(+) and its precursors to prevent Cognitive decline across Disease contexts. Nutrients. 2022;14(15).
28. Gasperi V, Sibilano M, Savini I, Catani MV. Niacin in the Central Nervous System: an update of Biological aspects and clinical applications. Int J Mol Sci. 2019;20(4).
29. Yang Y, Sauve AA. NAD(+) metabolism: Bioenergetics, signaling and manipulation for therapy. Biochim Biophys Acta. 2016;1864(12):1787–800.
30. Wu Y, Wang Y, Wu W, Yin D, Sun X, Guo X, et al. Effects of nicotinamide and sodium butyrate on meat quality and muscle ubiquitination degradation genes in broilers reared at a high stocking density. Poult Sci. 2020;99(3):1462–70.
31. Wu Y, Wang Y, Yin D, Wu W, Sun X, Zhang Y, et al. Effect of supplementation of nicotinamide and sodium butyrate on the growth performance, liver mitochondrial function and gut microbiota of broilers at high stocking density. Food Funct. 2019;10(11):7081–90.
32. Guo W, Liu J, Li W, Ma H, Gong Q, Kan X et al. Niacin alleviates dairy cow mastitis by regulating the GPR109A/AMPK/NRF2 signaling pathway. Int J Mol Sci. 2020;21(9).
33. Holecek M. Influence of Histidine Administration on Ammonia and amino acid metabolism: a review. Physiol Res. 2020;69(4):555–64.
34. Moro J, Tome D, Schmidely P, Demersay TC, Azzout-Marniche D. Histidine: a systematic review on metabolism and physiological effects in Human and different animal species. Nutrients. 2020;12(5).
35. Holecek M. Histidine in Health and Disease: metabolism, physiological importance, and use as a supplement. Nutrients. 2020;12(3).
36. Wang H, Cao L, Logue CM, Barbieri NL, Nolan LK, Lin J. Evaluation of immunogenicity and efficacy of the enterobactin conjugate vaccine in protecting chickens from colibacillosis. Vaccine. 2023;41(4):930–7.
37. Zhong Y, Li L, Chen W, Xing D, Wu X. Effects of Ilicis Chinensis folium extract supplementation on growth performance, serum parameters, intestinal morphology, and antioxidant capacity of broiler chickens. BMC Vet Res. 2023;19(1):94.
38. Arafat N, Abd El Rahman S, Naguib D, El-Shafei RA, Abdo W, Eladl AH. Co-infection of Salmonella enteritidis with H9N2 avian influenza virus in chickens. Avian Pathol. 2020;49(5):496–506.

Publisher's note